Application of Fluorescence Spectroscopy To Study the State of Water in Aerosols

Man Yee Choi, Chak K. Chan,* and Yun-Hong Zhang

Department of Chemical Engineering, Hong Kong University of Science and Technology, Clear Water Bay, Kowloon, Hong Kong

Received: May 30, 2003; In Final Form: December 16, 2003

The knowledge of the state of water molecules, particularly the amounts of solvated water and free water in aqueous droplets, is valuable in understanding the hydration properties of atmospheric aerosols. A novel technique combining the use of an electrodynamic balance and a fluorescence dye, 8-hydroxyl-1,3,6-pyrenetrisulfonate (pyranine), was used to study the state of the water molecules in single levitated aqueous droplets from subsaturation to supersaturation concentrations. The steady-state fluorescence spectra of sucrose, glucose, and NaCl solutions doped with 100 ppm pyranine were measured. The fluorescence emission of pyranine is sensitive to the proton-transfer capacity of its microenvironment. When excited by radiation at around 345 nm, pyranine fluoresces and the spectrum consists of two peaks, one at about 440 nm and the other at about 510 nm, which correspond to the presence of solvated and free water, respectively. The fluorescence peak intensity ratios of the 440-nm peak to the 510-nm peak and the hygroscopic measurements were used to calculate the amounts of solvated and free water in the droplets as a function of relative humidity. The amount of free water equals the amount of solvated water when crystallization or saturation (for noncrystallizating chemicals) occurs. Imaging analysis has revealed that the solvated to free water ratio oscillates within the droplets, which indicates the spatial heterogeneity of aqueous droplets. This study demonstrates that fluorescence spectroscopy is a unique tool in understanding the hydration properties, the efflorescence, and the structural heterogeneity of aqueous droplets.

Introduction

Atmospheric aerosols have a direct impact on the earth's radiation balance,[1] visibility degradation,[2−4] air pollution,[5] as well as human health.[6] Of central importance to these effects is the hygroscopic nature, i.e., the ability to absorb and evaporate water, of the atmospheric aerosols as they undergo size changes and phase transitions in moist air. The phase transformation of aerosols drastically alters their light-scattering properties[7,8] as well as their reactivity, such as the oxidation of SO_2(g) to SO_4^{2-}(aq) and the hydrolysis of N_2O_5 (ref 9). The reaction rate of sea salt aerosols with NO_2 also increases with increasing NO_2 pressure and relative humidity (RH) (ref 10).

In general, existing thermodynamic models[11−13] have been found to be acceptable for the prediction of the water activities of multicomponent inorganic aqueous aerosols in the troposphere. However, the phase transitions, especially the efflorescence, of atmospheric aerosols are much less understood. Since an aqueous aerosol is saturated or perhaps supersaturated when it effloresces, the molecular interaction between the water in the form of solvated water and the solute is expected to be very strong. Zhang and Chan[14] investigated the relationship between the solute and water interactions and the hygroscopicity of single levitated aqueous droplets of several metal sulfates compounds and $(NH_4)_2SO_4$ by Raman spectroscopy. They found that, at high concentrations, the chemical interactions between water molecules, sulfate ions, and the countercations are significant and lead to the formation of contact ion pairs, which hinders the mass transfer of water and affects the crystallization process in $MgSO_4$ and its mixtures with Na_2SO_4. The knowledge of the change of the state of water as the droplets become supersaturated and finally effloresce provides information valuable to understanding the hygroscopic properties and efflorescence of atmospheric aerosols. Unfortunately, there is little work reported in the literature addressing this issue.

This work aims at characterizing the state of water (solvated water vs free water) in supersaturated aerosols. Solvated and free water refer to the water molecules that interact directly with ions and those in the bulk water phase interacting with other free water, respectively. By combining two novel techniques, single-particle levitation using an electrodynamic balance (EDB), and the use of a fluorescence dye tracer, pyranine, the amounts of free water and solvated water in supersaturated solutions are determined. In this paper, we first describe the experimental system and the measurements of sucrose and glucose solutions, for which spectroscopic data of bulk solutions are available in the literature. Next, we investigate the changes of the state of water molecules in droplets of NaCl, one of the most commonly found inorganic compounds in atmospheric aerosols. The spatial distributions of the state of water in these droplets are also presented. Notably, spatial heterogeneity of the ratio of solvated to free water was found.

Method

The principle of the EDB has been well documented[17] and therefore is not described in detail here. Briefly, the EDB is an ideal device for studying supersaturated solutions because the particles in an EDB are not in contact with any foreign surface and thus the heterogeneous nucleation of solutions is suppressed. In a combination of ac and dc fields, a single charged particle of about 20 μm in diameter is trapped. Particles are generated by a piezoelectric particle generator (Uni-Photon Inc., model

* Author to whom correspondence may be addressed. E-mail: keckchan@ust.hk. Tel.: (852) 2358-7124. Fax: (852) 2358-0054.

10.1021/jp0355049 CCC: $27.50
Published on Web 01/24/2004

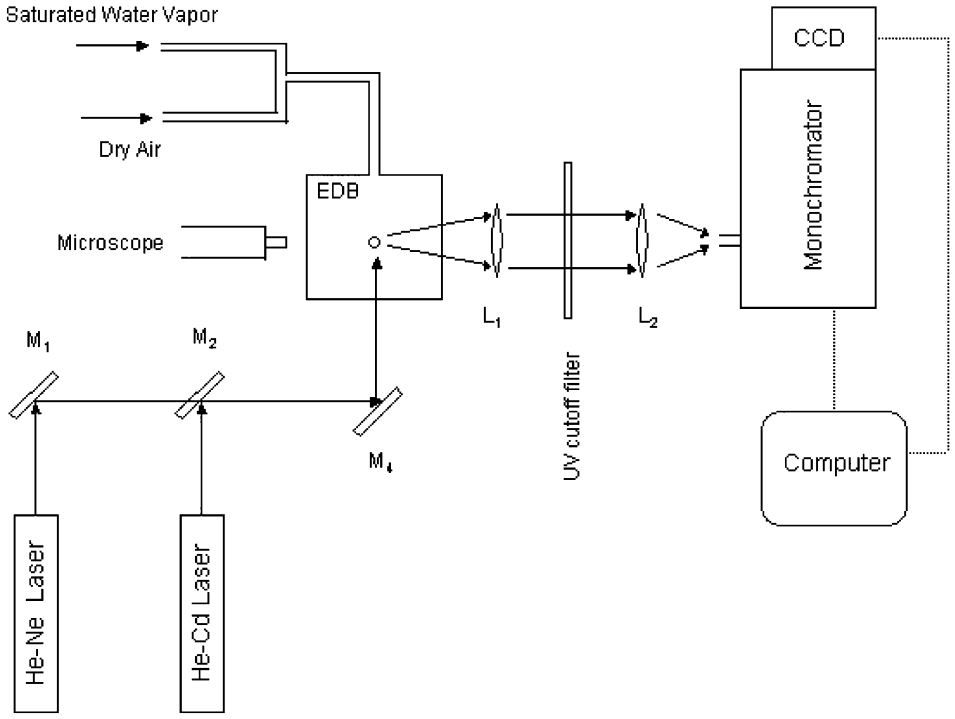

Figure 1. Schematic diagram of the single-particle fluorescence-spectroscopy system. M and L represent mirror and lens, respectively.

201) and charged by induction. The electrostatic force acting on the particle imposed by the dc voltage balances the weight of the particle and keeps the particle at the center of the balance. The mass of the particle equilibrated at different RH is proportional to the dc balancing voltage. The mfs (mass fraction of solute, defined as the mass of the solute on a dry basis over the mass of the solution) of the particle can be calculated from the dc voltage.

The RH of the feed air to the EDB was controlled by varying the mixing ratio of a stream of dry air and another of water-saturated air. The RH value was determined by a dew-point hygrometer (EG&G DewPrime, model 2000). Each particle was equilibrated with its ambient environment within an hour. The feed air was momentarily stopped when the dc balancing voltage and the fluorescence spectrum were measured. When the particle is equilibrated with its surrounding environment, the water activity (a_w) of the particle is related to the ambient RH by a_w = RH/100. The Kelvin effect for the correction of vapor pressure due to curvature of the droplet can be neglected for particles larger than 0.5 μm.

A fluorescence spectroscopy system consisting of a He−Cd laser (Kimmon IK3151R-E, CW = 325 nm, maximum power = 200 mW) and a 0.5-m monochromator (Acton SpectraPro 500) attached to a CCD (Andor Technology DV420-OE) was integrated with the EDB system, as shown in Figure 1. A pair of achromatic lenses, which are needed to minimize chromatic and spherical aberrations and coma due to the broad fluorescence spectra, was used to focus the 90° scattering of the levitated droplet in the EDB onto the slit of the monochromator. A 320-nm UV cutoff filter was placed between the two lenses to remove the strong Rayleigh scattering. A 150 g/mm grating was selected. The integration time of each spectrum was 20 s. All measurements were made at ambient temperatures of 22−24 °C. For each individual measurement, the temperature varied less than 0.5 °C. Deviations in the water activity, the saturation concentration, and the fluorescence spectra within such small temperature changes are not significant. Since it is possible for negatively charged particles to lose electrons upon UV irradiation, each particle was discarded after 3−4 fluorescence measurements. Positively charged particles were also studied, and the results from negatively and positively charged particles were consistent. The bulk data were measured by the same spectroscopic system without the collection optics for the levitated particles. Instead, a quartz cuvette containing the bulk solution at the prescribed concentration was used, and 90° scattering from the solution was collected by an optical fiber that was directly coupled to the slit of the monochromator.

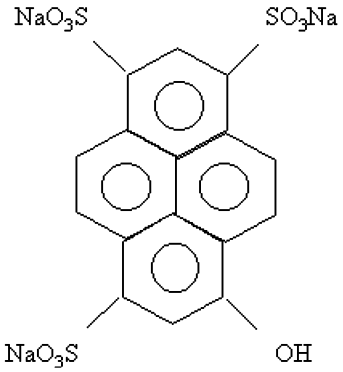

Figure 2. Chemical structure of pyranine.

Pyranine (8-hydroxy-1,3,6-pyrenetrisulfonate), whose molecular structure is shown in Figure 2, is a water-soluble probe with a polarity-dependent equilibrium between two excited states that fluoresce. The photochemistry of pyranine has been well characterized by Kondo et al.[18] When pyranine is dissolved in water, the three sulfonate groups are completely dissociated but the dissociation of the hydroxyl proton depends on the proton-transfer ability of the microenvironment. Upon excitation at around 345 nm, pyranine fluoresces and emits a broad spectrum, which generally consists of two peaks, one at around 440 nm and the other at around 510 nm. These two peaks correspond to the emissions from the excited protonated form and the excited deprotonated form of pyranine, respectively (Figure 3). Free water molecules in aqueous solutions facilitate the proton

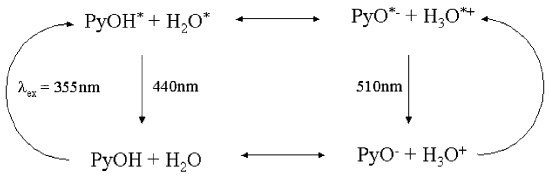

Figure 3. The fluorescence emission equilibrium of pyranine.

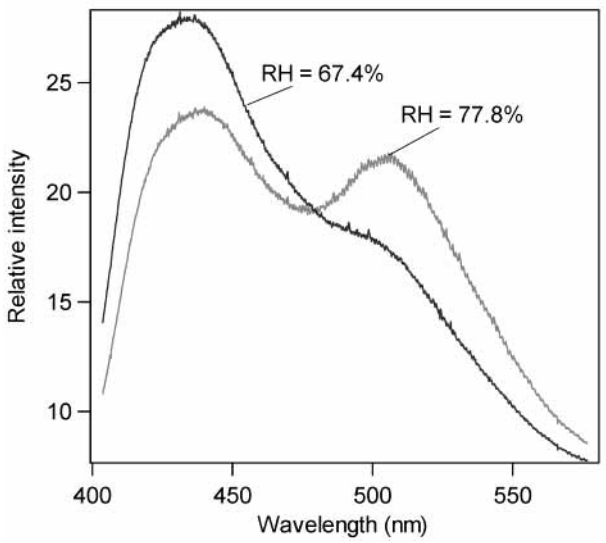

Figure 4. The emission spectrum of a levitated sucrose droplet doped with 100 ppm (1.9×10^{-4} M) pyranine at RH = 67.4 and 77.8%.

exchange and therefore promote the deprotonated form. In the presence of free water molecules, the protonated form does not exist until the pH of the solution is lower than 3. In contrast, solvated water molecules do not support proton exchange. In the absence of free water, the proton exchange cannot take place, which results in the protonated form. The protonated form can exist in concentrated or supersaturated solutions. The peak intensity ratio (PIR) of the 440-nm peak to the 510-nm peak (PIR = I_{440}/I_{510}) in the fluorescence spectra is therefore an indicator of the amount of solvated water over the amount of free water. An advantage of using the peak ratio method is that it eliminates the effects of certain measurement variables such as laser intensity, collection optics, and the pyranine concentration. The CCD response was almost the same at 440 and 510 nm, and therefore data correction was not needed. Because of its unique characteristics, pyranine has been used to study the water content of sol−gels from the water/alcohol ratio,[19−21] in situ pH analysis,[22] the structures of reversed micelles,[18] and the state of water in supersaturated solutions.[23,24] In our study, stock solutions of 100 ppm (1.9×10^{-4} M) pyranine were prepared using 18 Mohm water and pyranine (98% purity) from Acros Organics without further purification. The effects of the trace amounts of pyranine on the hygroscopic and efflorescence behaviors of the chemicals have been confirmed to be negligible in this study.

Results and Discussion

Validation of the Single-Particle Fluorescence-Sectroscopy System. Figure 4 shows the fluorescence spectra of levitated sucrose particles equilibrated at RH = 67.4 and 77.8%. The 440-nm peak increases while the 510-nm peak decreases when RH decreases from 77.8 to 67.4%. The mole ratio of the total water to solute at a given RH is calculated from the mfs. With the PIR calculated from the 440-nm and 510-nm peak intensities and the mfs of the levitated particles, the molar ratios of the free and solvated water molecules to solute at any RH were determined. Figure 5 shows the mole ratios of total water, free water, and solvated water to sucrose as a function of mfs from both bulk and single-particle studies, indicated by filled and open symbols, respectively. A similar plot for glucose is shown in Figure 6. The measurements using positively and negatively charged particles are consistent.

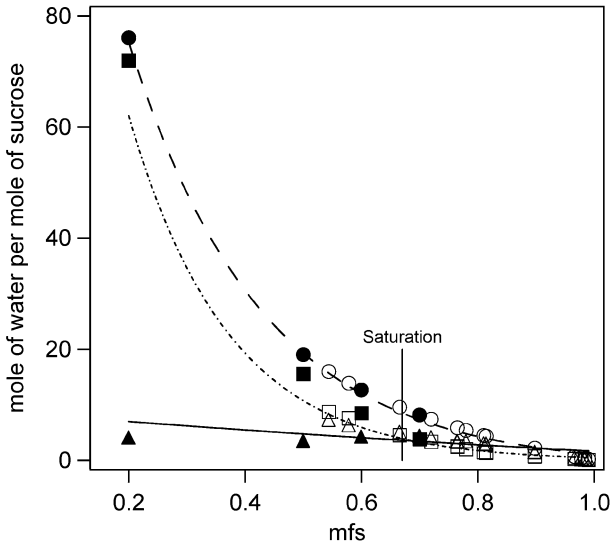

Figure 5. Moles of total, free, and solvated water per mol of sucrose as a function of *mfs* in bulk and single-particle measurements. ●, total water in bulk measurements; ○, total water in single-particle measurements; ■, free water in bulk measurements; □, free water in single-particle measurements; ▲, solvated water in bulk measurements; △, solvated water in single-particle measurements. The vertical line indicates the saturation concentration from Ruegg and Blanc.[25] Dashed line, exponential equation fitting for the amount of total water; dot-dashed line, exponential equation fitting for the amount of free water; line, exponential equation fitting for the amount of solvated water.

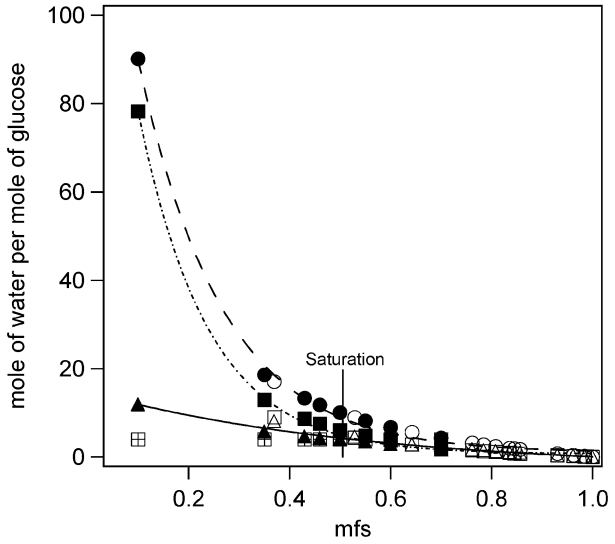

Figure 6. Moles of total, free and solvated water per mole of glucose as a function of *mfs* in bulk and single-particle measurements. ●, total water in bulk measurements; ○, total water in single-particle measurements; ■, free water in bulk measurements; □, free water in single-particle measurements; ▲, solvated water in bulk measurements; △, solvated water in single-particle measurements; ⊞, chemically associated water in bulk measurements. The vertical line indicates the saturation concentration from Ruegg and Blanc.[25] Dashed line, exponential equation fitting for the amount of total water; dot-dashed line, exponential equation fitting for the amount of free water; line, exponential equation fitting for the amount of solvated water.

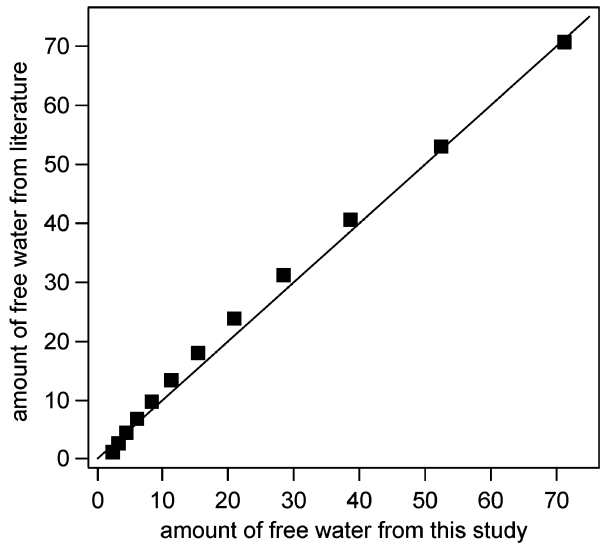

Figure 7. Comparison of literature values and experimental measurements in the mole of free water per mol of sucrose at the same mfs. The literature data are taken from Chakraborty and Berglund.[23] ■, mol of free water per mol of sucrose. The solid line indicates the 45° line.

According to Figures 5 and 6, the amounts of total and free water decrease exponentially with increasing mfs (i.e., decreasing RH), which is consistent with the observation by Chakraborty and Berglund.[23] Figure 7 shows that our measurements (bulk and single particles) are in good agreement with the data from Chakraborty and Berglund[23] for the free water of sucrose. In Figures 5 and 6, the solid lines indicate the exponential equation fittings of the mole ratios of total, free, and solvated water to solute. Each mol of sucrose and glucose is solvated by about 6 and 4 mol of water, respectively, at the saturation point (saturation mfs = 0.67 and 0.51 for sucrose and glucose, respectively, from Ruegg and Blanc),[25] which is also in agreement with the results from Chakraborty and Berglund.[23]

It is interesting to note that the mole ratios of free and solvated water of sucrose gradually become the same when the concentration increases to saturation, as demonstrated by both the experimental measurements and the intersection of the exponential fittings. Chakraborty and Berglund[23] also made the same observation in their bulk sucrose and fructose measurements. They proposed that the free water is responsible for maintaining a structurally stable saturated solution and the intersection point indicates an equilibrium between the solvated solute and free water, beyond which it is energetically unfavorable to add more solute to the solution without supplying external energy. However, they found that the amounts of free water and solvated water are not the same in the case of glucose and lactose. They explained this inconsistency through the presence of water chemically associated with the glucose and lactose hydroxyl groups, apart from free and solvated water. These chemically associated water molecules exchange protons at an intermediate rate, slower than that of free water but faster than that of solvated water. Pyranine responds to these water molecules as "free water" in terms of proton transfer.

In this study, the amounts of free and solvated water in bulk glucose solutions are equal at saturation only after subtracting the amount of chemically associated water (4 per molecule of glucose)[23] from the amount of free water. This suggests that the water molecules chemically associated with glucose are present in the bulk samples. However, in the single-particle studies, the amounts of free and solvated water are equal for both sucrose and glucose solutions at saturation, without the subtraction of chemically associated water, as shown in Figures 5 and 6. This suggests that the "chemically associated water" is absent in the single glucose droplets.

The main structure of glucose is a six-membered ring that carries one hydroxymethyl and four hydroxyl groups. It has two anomeric forms, α and β, which differ by the orientation (axial or equatorial with respect to the ring) of one of the hydroxyl groups. Molteni and Parrinello[26] performed ab initio molecular dynamics simulations on aqueous glucose solutions and found that the crucial anomeric oxygen has different solvation properties in the β and α anomers. The β anomer allows water molecules to flow in a disorderly manner around its anomeric site, while the α anomer tends to bind them more tightly. Therefore, the conformation of glucose is also important in affecting the state of water around the glucose molecules, and the presence of "chemically associated water" is most likely due to the α anomer. However, the precise structure of water around either anomer is still unknown,[27] and the literature results on the solvation of the two anomers are somewhat contradictory,[28] due to the small free-energy difference between the α and β anomers. The differences in the solvation pattern and molecular conformation of glucose solution between bulk solutions and single particles and the actual reason for the absence of "chemically associated water" in single glucose droplets are still not elucidated. Nevertheless, the anomeric equilibrium likely plays an important role in affecting the solvation pattern of aqueous glucose solutions.

Overall, the single-particle fluorescence-spectroscopy results of sucrose and glucose are in good agreement with the bulk measurements in the literature.[23] When the amounts of solvated and free water are equal, the droplets reach their saturation concentrations. Empirical exponential fittings of the amounts of solvated and free water appear to be useful to predict the saturation concentration. Although efflorescence of glucose and sucrose droplets was not observed at saturation conditions, these measurements suggest that the equality of the concentrations of solvated and free water is associated with the saturation condition, at which structural changes of the interactions of solute and water likely exist despite the absence of efflorescence. The application of pyranine to probe the state of water of crystallizing droplets and the onset of crystallization will be presented using NaCl as an example in the following section.

NaCl Solutions. Figure 8 shows the mole ratios of total, free, and solvated water to NaCl as a function of mfs in both bulk and single-particle measurements (indicated by filled and open symbols, respectively). As with sucrose and glucose, the mole ratios of total and free water to solute decrease exponentially with increasing mfs. The trace amount of added pyranine does not change the hygroscopic properties of NaCl, as the particle crystallizes at an RH similar to the literature crystallization RH (CRH) value of 48.4% (at mfs = 0.43, e.g., ref 29). The mole ratio of the solvated water to NaCl in the levitated particles decreases from about 4.8 at mfs = 0.18 to about 2 before crystallization. The structure of the solvated solute may exist in a form related to $NaCl{\cdot}2H_2O$ (dihydrate), which is stable at temperatures lower than 0°C. At the crystallization mfs, the ratios of free and solvated water are the same, indicating that the equality of their concentrations is a condition associated with phase transformation.

The solvation number of Na^+ ions has generally been reported to be 5 or 6 for 1 M solutions in the literature.[30−33] However, the solvation number is measurement-method and concentration dependent. For example, Na^+ ions have been found to solvate with 4−8 water molecules at water−salt molar ratios of 10.2−

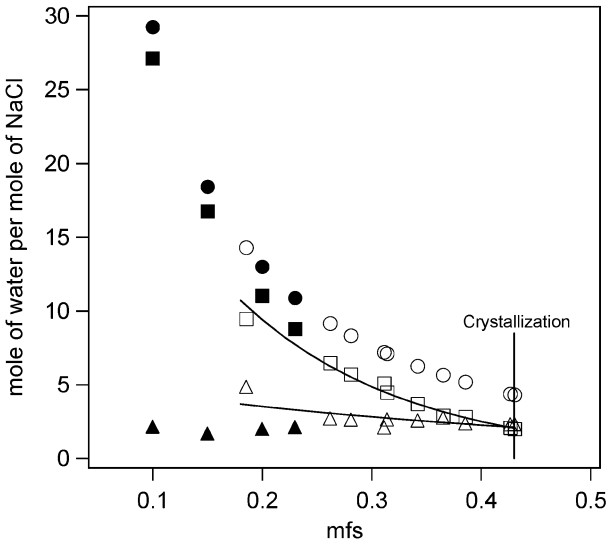

Figure 8. Moles of total, free, and solvated water per mole of NaCl as a function of *mfs* in bulk and single-particle measurements. ●, total water in bulk measurements; ○, total water in single-particle measurements; ■, free water in bulk measurements; □, free water in single-particle measurements; ▲, solvated water in bulk measurements; △, solvated water in single-particle measurements. The vertical line indicates the typical crystallization *mfs* from Cohen et al.[29] Line, exponential equation fitting for the amount of free and solvated water.

54.3 through experimental measurements and with 2−7 water molecules at water−salt molar ratios of 7.9−100 through computer simulations.[34] Zhu and Robinson[35] and Degreve and Silva[36] reported a solvation number of 6 for Cl^- ions. Therefore, under supersaturation conditions, Na^+ and Cl^- ions are only partially solvated, with the solvation number much lower than that measured in bulk studies. Significant ion pairing, including the formation of solvent-separated ion pairs and even direct contact ion pairs, is expected in these solutions.[15] The formation of contact ion pairs affects the morphology of the solid formed as a result of efflorescence of supersaturated droplets, as will be discussed later.

However, unlike the measurements of sucrose and glucose, the single-particle measurements and bulk measurements of NaCl are not consistent. As shown in Figure 8, the amount of free water in single-particle measurements is slightly less (about 20%) than that in bulk measurements at the same mfs (concentration), i.e., the single-particle measurements have higher solvated to free water ratios than do the bulk studies. Moreover, the amounts of free and solvated water in the bulk measurements are not equal at the bulk saturation point (mfs = 0.266). In bulk studies, even if there exists enough free water to maintain a stable hydration structure, the presence of foreign surfaces induces crystallization.

Spatial Heterogeneity of Droplets. Parts a and b of Figure 9 show the PIR of sucrose and glucose droplets at RH = 80 and 70% as a function of pixel number, which represents the location from the bottom to the top of a droplet. The PIR values were recorded with the CCD in the imaging mode. Pixels 1 and 35 (18 for glucose) represent the bottom and top edges of the droplet, respectively. The differences in the PIR between RH = 80 and 70% are small. In both cases, the solvated to free water ratios have oscillations within the droplet. Since the patterns of the oscillating PIR at different RH are almost the same, these oscillations are not due to Mie morphological resonances, which would produce significantly different spectra even at very small changes in particle diameter.[37] It is interesting to note that the PIR values are not symmetric. We have

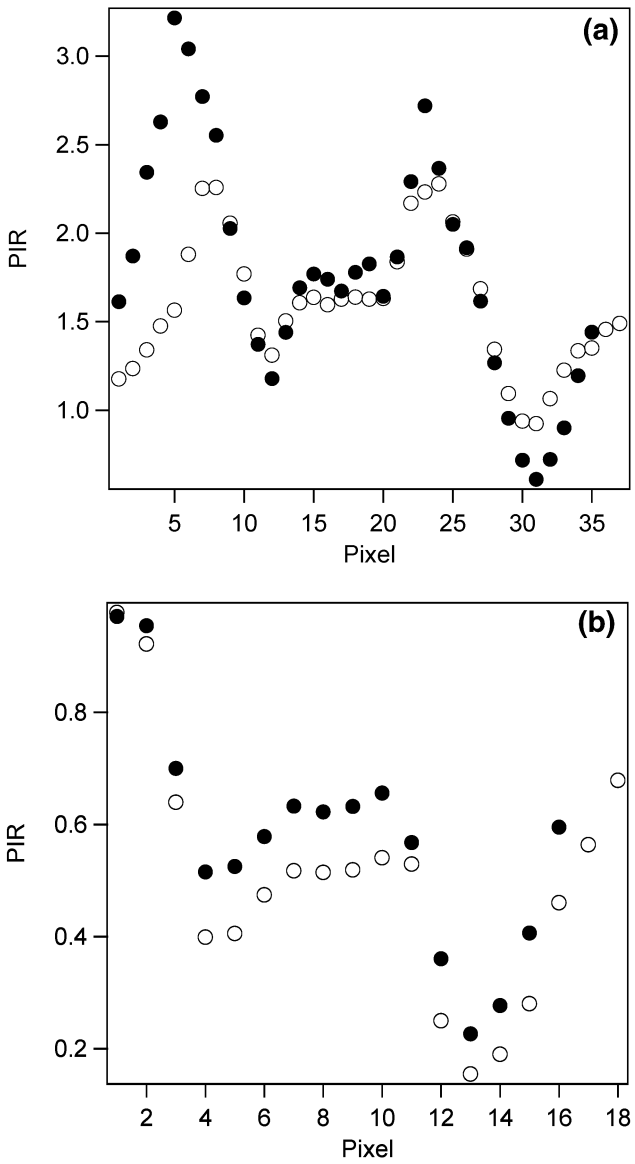

Figure 9. (a) The PIR of sucrose droplet along the equator of the droplet. ○, RH = 80%; ●, RH = 70%. (b) The PIR of glucose droplet along the equator of the droplet. ○, PIR at RH = 80%; ●, PIR at RH = 70%.

confirmed that it is not an optical effect since the imaging spectra of sucrose droplets are independent of whether the droplets are irradiated by the laser from above or below. Figure 10 shows the fluorescence spectra and the PIR values of a NaCl droplet at RH = 80 and 70%. Similar to the sugar droplets, there are oscillations of PIR, but the PIR near the surface is higher than that near the center of the droplet.

Recently, the spatial distribution of solutes at the water/air interface has received much attention. In particular, Docoslis et al.[38] reported a depletion of sugar molecules near the water/air interface, which would result in a higher solvation number (i.e., higher PIR) near the surface. Conversely, preferential enrichment of chloride ions near the surface, as suggested in recent studies in association with the enhanced role of sea-salt aerosols in gas-phase atmospheric chemistry, would result in a lower PIR near the surface on average.[39−41] However, the oscillations of the PIR observed in our measurements infer that the structures of the aqueous droplets are probably more complex than a thin surface layer of a few nanometers deep with solute enrichment/depletion surrounding the bulk of the droplet.

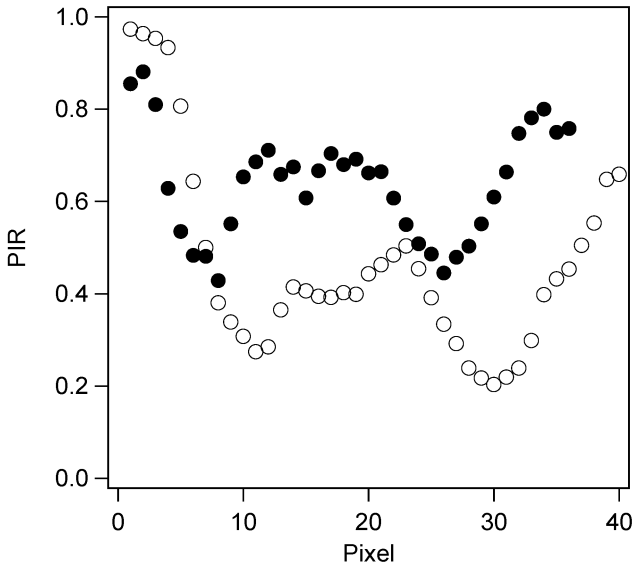

Figure 10. The PIR of a NaCl droplet along the equator of the droplet. ○, PIR at RH = 80%; ●, PIR at RH = 70%.

Formation of Contact Ion Pairs at High Supersaturation. At high concentrations, ions in solutions tend to form ion pairs because of insufficient free water molecules to separate and solvate the ions. They can exist in the form of solvent-separated ion pairs or direct contact ion pairs at very high concentrations, e.g., at supersaturation. Jungwirth and Tobias[15] predicted that Cl^- can occupy a significant fraction of the surface and calculated that 54% of the Cl^- ions are paired with Na^+ ions at the air−solution interface of an aqueous NaCl slab at 6.1 M, the bulk saturation concentration. Many more Cl^- ions are expected to form ion pairs near the surface at supersaturation. During crystallization, if the mass transfer of water or solute within a particle is hindered, e.g., due to the presence of viscous compounds such as glycerol[42] or a very rapid evaporation at high temperatures,[43] these Na^+-Cl^- ion pairs cannot diffuse into the interior of the particle, which ultimately leads to the formation of a solid NaCl crust. Choi and Chan[42] studied the effect of organics on the hygroscopic properties of NaCl and $(NH_4)_2SO_4$ and found that the addition of glycerol, a species that absorbs water even at RH < 20%, does not affect the deliquescence RH of NaCl and $(NH_4)_2SO_4$. If glycerol were at the surface of the "dried" levitated particle, the mixed particle would absorb water even at RH much lower than the deliquescence RH of pure NaCl (70−75% from Tang and Munkelwitz).[44] Because of the formation of a solid NaCl crust that traps the glycerol, water vapor can only interact with the solid NaCl crust and thus the particle does not absorb water until the deliquescence *RH* of NaCl is reached.

Conclusions

This paper presents a novel approach to understanding the hygroscopic properties of aerosols, using single-particle fluorescence spectroscopy to probe the state of water molecules in diluted to supersaturated aerosols. The results show that structural changes occur (e.g., saturation for noncrystallizing species and efflorescence for crystallizing species) when the amounts of solvated and free water are equal. It appears that the condition of more free water than solvated water is the criterion for maintaining a stable solvation structure. This study also shows that the solvation pattern of supersaturated droplets differs significantly from that of subsaturated solutions. Therefore, the phase transition of supersaturated aerosols is complex and may not be predicted from bulk studies. Imaging results of the sugar and NaCl droplets show that the droplets are not structurally homogeneous. Surface enrichment of chloride in NaCl droplets, as currently understood in the literature, cannot explain the observation. Nevertheless, our results clearly show the spatial heterogeneity in droplets, which may be important to understanding the heterogeneous chemistry of atmospheric aerosols.

Acknowledgment. This work was supported by the Research Grants Council of the Hong Kong Special Administrative Region, China (Project No. HKUST6042/01P). Y.H.Z., on leave from the Beijing Institute of Technology, China, was supported by the HKUST PDF Grant.

References and Notes

(1) Intergovernmental Panel on Climate Change (IPCC), *Climate change*, Cambridge University Press: New York, 1995.
(2) Sloane, C. S. *Atmos. Environ.* **1984**, *18*, 871.
(3) Sloane, C. S.; White, W. H. *Environ. Sci. Technol.* **1986**, 20, 760.
(4) Eldering, A.; Larson, S. M.; Hall, J. R.; Hussey, K. J.; Cass, G. R. *Environ. Sci. Technol.* **1993**, 27, 626.
(5) Seinfeld, J. H. *Science* **1989**, *243*, 745.
(6) Dockery, D. W.; Pope, C. A., III; Xu, X.; Spengler, J. D.; Ware, J. H.; Fay, M. E.; Ferris, B. G., Jr.; Speizer, F. E. *New Engl. J. Med.* **1993**, 329, 1753.
(7) Tang, I. N. *J. Geophys. Res.* **1996**, *101*, 19245.
(8) Malm, W. C.; Day, D. E. *Atmos. Environ.* **2001**, *35*, 2848.
(9) Martin, S. T. *Chem. Rev.* **2000**, *100*, 3403.
(10) Weis, D. D.; Ewing, G. E. *J. Phys. Chem. A* **1999**, *103* (25), 4865.
(11) Kim, Y. P.; Seinfeld, J. H.; Saxena, P. *Aerosol Sci. Technol.* **1993**, *19*, 157.
(12) Kim, Y. P.; Seinfeld, J. H. *Aerosol Sci. Technol.* **1995**, *22*, 93.
(13) Clegg, S. L.; Brimblecombe, P.; Wexler, A. S. *J. Phys. Chem. A* **1998**, *102*, 2137.
(14) Zhang, Y. H.; Chan, C. K. *J. Phys. Chem. A* **2002**, *106*, 285.
(15) Jungwirth, P.; Tobias, D. J. *J. Phys. Chem. B* **2002**, *106*, 6361.
(16) Stuart, S. J.; Berne, B. J. *J. Phys. Chem. A* **1999**, *103*, 10300.
(17) Davis, E. J. *Aerosol Sci. Technol.* **1997**, *26*, 212.
(18) Kondo, H.; Miwa, I.; Sunamoto, J. *J. Phys. Chem.* **1982**, *86*, 4826.
(19) Pouxviel, J. C.; Dunn, B.; Zink, J. I. *J. Phys. Chem.* **1989**, *93*, 2134.
(20) Nishida, F.; McKiernan, J. M.; Dunn, B.; Zink, J. I.; Brinker, C. J.; Hurd, A. J. *J. Am. Ceram. Soc.* **1995**, *78* (6), 1640.
(21) Wasiucionek, M.; Breiter, M. W. *J. Non-Cryst. Solids* **1997**, *220*, 52.
(22) Samuel, J.; Strinkovski, A.; Shalom, S.; Liberman, K.; Ottolenghi, M.; Svnir, D.; Lewis, A. *Mater. Lett.* **1994**, 431.
(23) Chakraborty R.; Berglund, K. A. *J. Cryst. Growth* **1992**, *125*, 81.
(24) Yedur, S. K.; Berglund, K. A. *Appl. Spectrosc.* **1996**, *50* (7), 866.
(25) Ruegg, M.; Blanc, B. *Lebensm.-Wiss. Technol.* **1989**, *14*, 1.
(26) Molteni, C.; Parrinello, M. *J. Am. Chem. Soc.* **1998**, *120*, 2168.
(27) Lewis, B. E.; Scjramm, V. L., *J. Am. Chem. Soc.* **2001**, *123*, 1327.
(28) Vaneijck, B. P.; Hooft, R. W. W.; Kroon, J. *J. Phys. Chem.* **1993**, *97* (46), 12093.
(29) Cohen, M. D.; Flagan, R. C.; Seinfeld, J. H. *J. Phys. Chem.* **1987**, *91*, 4563.
(30) Chitra, R.; Smith, P. E. *J. Phys. Chem. B* **2000**, *104*, 58854.
(31) Max, J.-J.; Chapados, C. *J. Chem. Phys.* **2001**, *115* (6), 2664.
(32) Brodskaya, E.; Lybuartsev, A. P.; Laaksonen, A. *J. Chem. Phys.* **2002**, *116* (18), 7879.
(33) Dillon, S. R.; Dougherty, R. C. *J. Phys. Chem. A* **2002**, *106* (34), 7647−7650.
(34) Ohtaki, H.; Radnal, T. *Chem. Rev.* **1993**, *93*, 1157.
(35) Zhu, S. B., Robinson, G. W. *J. Chem. Phys.* **1992**, *97* (6), 4336.
(36) Degreve, L.; da Silva, F. L. B. *J. Chem. Phys.* **1999**, *110* (6), 3070.
(37) Chan, C. K.; Flagan, R. C.; Seinfeld, J. H. *Appl. Opt.* **1990**, *30* (4), 459.
(38) Docoslis, A.; Giese, R. F.; van Oss, C. J. *Colloids Surf., B* **2000**, *19*, 147.
(39) Jungwirth, P. *J. Phys. Chem. A* **2000**, *104*, 145.
(40) Knipping, E. M.; Lakin, M. J.; Foster, K. L.; Jungwirth, P.; Tobias, D. J.; Gerber, R. B.; Dabdub, D.; Finlayson-Pitts, B. J. *Science* **2000**, *288*, 301.
(41) Seinfeld, J. H. *Science* **2000**, *288*, 285.
(42) Choi, M. Y.; Chan, C. K. *Environ. Sci. Technol.* **2002**, *36* (11), 2422.
(43) Lin, J. C.; Gentry, J. W. *Aerosol Sci. Technol.* **2003**, *37*, 15.
(44) Tang, I. N.; Munkelwitz, H. R. *J. Geophys. Res.* **1994**, *99*, 18801.